

# Collider Bounds on Indirect Dark Matter Searches: the $WW$ final state

Nicolas Lopez,<sup>1</sup> Linda M. Carpenter,<sup>2</sup> Randel Cotta,<sup>3</sup> Meghan Frate,<sup>3</sup> Ning Zhou,<sup>3</sup> and Daniel Whiteson<sup>3</sup>

<sup>1</sup>*Massachusetts Institute of Technology, Cambridge, MA*

<sup>2</sup>*The Ohio State University, Columbus, OH*

<sup>3</sup>*Department of Physics and Astronomy, University of California, Irvine, CA 92697*

We describe an effective theory of interaction between pairs of dark matter particles (denoted  $\chi$ ) and pairs of  $W$  bosons. Such an interaction could accomodate  $\chi\bar{\chi} \rightarrow WW$  processes, which are a major focus of indirect dark matter experiments, as well as  $pp \rightarrow W \rightarrow W\chi\bar{\chi}$  processes, which would predict excesses at the LHC in the  $W + \cancel{E}_T$  final-state. We reinterpret an ATLAS  $W + \cancel{E}_T$  analysis in the hadronic mode and translate the bounds to the space of indirect detection signals. We also reinterpret the  $W + \cancel{E}_T$  analysis in terms of graviton theory through the processes  $W \rightarrow WG$  and  $Z \rightarrow ZG$  in which  $G$  is invisible. Finally, the final state is interpreted in terms of a  $W'$  model where  $W' \rightarrow WZ$ , where  $W$  decays hadronically and  $Z$  decays to neutrinos.

PACS numbers:

## Introduction

It is well-established that dark matter makes up a significant fraction of the matter and energy density of the Universe [1, 2], but its particle nature and the form of its non-gravitational interactions remain important mysteries.

Dedicated experiments search for interactions between dark matter particles and quiet nuclei (called *direct detection* [3, 4]), or for dark matter annihilation in space leading to visible particles (*indirect detection* [5]). In addition, experiments at high-energy particle colliders play a complementary role, often with the greatest sensitivity for low-mass dark matter [6–9]. In order to analyze the collider data in the same framework as indirect- and direct-detection experiments, it is convenient to encapsulate our lack of knowledge of the form of the interaction between dark matter and the standard model as an effective field theory (EFT), in which the dark matter is fairly light and mediators are heavy enough to be integrated into four-point effective vertices [10–12] between quarks and dark matter particles.

At particle colliders, this interaction produces invisible pairs of dark matter particles ( $pp \rightarrow \chi\bar{\chi}$ ), and so relies on initial-state radiation of a visible object (jet, photon,  $Z$  boson, etc) in order to leave a visible detector signature (jet+ $\cancel{E}_T$ ,  $\gamma$ + $\cancel{E}_T$ ,  $Z$ + $\cancel{E}_T$ , etc). In these cases, initial-state radiation of a photon or  $Z$  boson is not as sensitive as radiation of a gluon [13] for theories in which dark matter interacts with quarks and gluons, but these channels have unique power to probe interactions between DM and photons or  $Z$  bosons, leading to effective vertices with two gauge bosons and two DM particles [14–18].

In this paper, we extend this line of thought to the  $W + \cancel{E}_T$  final state. We reinterpret the recent ATLAS analysis [19] which sets limits on theories of quark-DM effective interactions (see the top of Fig. 1) in terms of

theories of  $W$ -DM effective interactions (see the bottom of Fig. 1), working in an effective theory framework with a very simple parameter space.

This class of interactions is of particular interest as collider production of  $W + \cancel{E}_T$  via  $W \rightarrow W\chi\bar{\chi}$  is tied directly to the signal rates of indirect dark matter signals via  $\chi\bar{\chi} \rightarrow WW$ , allowing the comparison of LHC and indirect experiments in the parameter space of our new effective theory.

In addition, we point out that the collider  $W + \cancel{E}_T$  signature has broad sensitivity to other models which produce invisible particles. We demonstrate how this extends to graviton production in ADD [21] models, as well as exotic  $W'$  bosons [22].

## Dark Matter Models

In deriving bounds on effective theories of dark matter, we consider effective operators through which pairs of neutral stable particles (the DM) may couple to  $W$  bosons. We consider the most relevant such operators for both scalar and fermionic DM particles, denoted  $\chi$ .

Taking all operators of effective dimension 6 and 7, one finds that the DM couples to the square of the field strength tensors of the  $SU(2)$  gauge group through a variety of Lorentz structures. The most general dimension 6 operators involving scalar dark matter particles are:

$$\mathcal{L}_{B1+B2} = \frac{1}{\Lambda_{B1}^2} \bar{\phi}\phi F_1^{\mu\nu} F_{\mu\nu}^1 + \frac{1}{\Lambda_{B2}^2} \bar{\phi}\phi F_2^{\mu\nu} F_{\mu\nu}^2$$

and

$$\mathcal{L}_{B3+B4} = \frac{1}{\Lambda_{B3}^2} \bar{\phi}\phi F_1^{\mu\nu} \tilde{F}_{\mu\nu}^1 + \frac{1}{\Lambda_{B4}^2} \bar{\phi}\phi F_2^{\mu\nu} \tilde{F}_{\mu\nu}^2 \quad (1)$$

where  $F_i$ ,  $i = 1, 2$  are the Standard Model  $U(1)$  and  $SU(2)$  field strength tensors.  $\Lambda_{Bi}$  and  $\Lambda_{Ci}$  below are

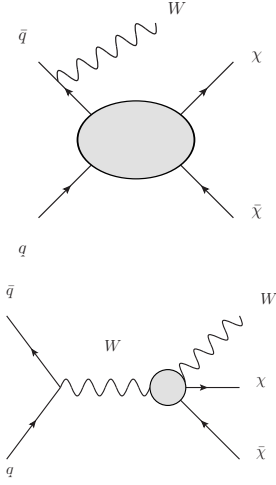


FIG. 1: Representative diagrams for production of dark matter pairs ( $\chi\bar{\chi}$ ) associated with a  $W$  boson in theories where dark matter interacts with quarks (top) or directly with weak boson pairs (bottom). The latter are those that we consider in this work.

the effective cut-off scales of the operators, following the notation of Ref. [18]. In the second set of operators, the dual field strength tensor appears.

Generic operators in which fermionic DM can couple to  $SU(2)$  bosons in gauge-invariant fashion start at dimension 7. There are now more operators to consider due to the Lorentz structure of the DM bilinear:

$$\begin{aligned}\mathcal{L}_{C1+C2} &= \frac{1}{\Lambda_{C1}^3} \bar{\chi}\chi F_1^{\mu\nu} F_{\mu\nu}^1 + \frac{1}{\Lambda_{C2}^3} \bar{\chi}\chi F_2^{\mu\nu} F_{\mu\nu}^2, \\ \mathcal{L}_{C3+C4} &= \frac{1}{\Lambda_{C3}^3} \bar{\chi}\chi F_1^{\mu\nu} \tilde{F}_{\mu\nu}^1 + \frac{1}{\Lambda_{C4}^3} \bar{\chi}\chi F_2^{\mu\nu} \tilde{F}_{\mu\nu}^2\end{aligned}\quad (2)$$

as well as

$$\begin{aligned}\mathcal{L}_{C5+C6} &= \frac{1}{\Lambda_{C5}^3} \bar{\chi}\gamma^5\chi F_1^{\mu\nu} F_{\mu\nu}^1 + \frac{1}{\Lambda_{C6}^3} \bar{\chi}\gamma^5\chi F_2^{\mu\nu} F_{\mu\nu}^2, \\ \mathcal{L}_{C7+C8} &= \frac{1}{\Lambda_{C7}^3} \bar{\chi}\gamma^5\chi F_1^{\mu\nu} \tilde{F}_{\mu\nu}^1 + \frac{1}{\Lambda_{C8}^3} \bar{\chi}\gamma^5\chi F_2^{\mu\nu} \tilde{F}_{\mu\nu}^2,\end{aligned}\quad (3)$$

Importantly, however, the  $SU(2)$  invariance of the dimension 6,7 operators mentioned above implies precise relationships between operators connecting the DM particles with various electroweak gauge bosons of the SM.

These couplings are presented using a modified notation which nicely demonstrates how DM couplings to gauge bosons are related by gauge invariance. For effective operators involving  $\mathcal{L}_{Cn+Cn+1}$  we define  $(1/\Lambda_{Cn}^3) = k_1/\Lambda^3$  and  $(1/\Lambda_{Cn+1}^3) = k_2/\Lambda^3$ . Similarly, for any effective operators involving  $\mathcal{L}_{Bn+Bn+1}$  we define  $(1/\Lambda_{Bn}^2) = k_1/\Lambda^2$  and  $(1/\Lambda_{Bn+1}^2) = k_2/\Lambda^2$ . The DM couplings to

pairs of electro-weak bosons are thus given by:

$$\begin{aligned}g_{WW} &= \frac{2k_2}{s_w^2\Lambda^{2-3}} \\ g_{ZZ} &= \frac{1}{4s_w^2\Lambda^{2-3}} \left( \frac{k_1 s_w^2}{c_w^2} + \frac{k_2 c_w^2}{s_w^2} \right) \\ g_{\gamma\gamma} &= \frac{1}{4c_w^2} \frac{k_1 + k_2}{\Lambda^{2-3}} \\ g_{Z\gamma} &= \frac{1}{2s_w c_w \Lambda^{2-3}} \left( \frac{k_2}{s_w^2} - \frac{k_1}{c_w^2} \right)\end{aligned}\quad (4)$$

where  $s_w$  and  $c_w$  are the sine and cosine of the weak mixing angle, respectively. In all cases the overall operator coefficient coupling DM particle pairs to pairs of  $W$  bosons depends only on a single parameter  $k_2/\Lambda^2$  (or  $k_2/\Lambda^3$  depending on the dimension of the operator). Assuming then that a single operator structure dominates, the overall production cross section of  $pp \rightarrow W\chi\chi$  will depend only on two parameters, the mass of the dark matter particle and the overall coefficient  $k_2/\Lambda^{2,3}$ . A prediction of a specific number of  $W + \cancel{E}_T$  events also implies correlated predictions for numbers of events in other mono-boson channels as well.

### Heavy Boson Models

In the case of gravitons, we consider the ADD model of extra dimensions[21], which is a proposed solution to the hierarchy problem in which there are  $\delta$  extra dimensions of submillimeter size through which gravity propagates, with all other Standard Model (SM) fields localized on a higher dimensional 3 space brane. In this model, the reduced Planck scale  $M_D$ , where gravity becomes strong, is far below the 4-D Planck scale  $M_P \sim 10^{18}$  GeV. The reduced Planck scale is set by the number and radius of the extra dimensions.  $M_P^2 = R^\delta M_D^{2+\delta}$  where  $R$  is the radius of extra dimensions. This model contains a series of Kaluza-Klein (KK) excitation states of graviton with masses  $m_n = n/R$ . Although each KK graviton has gravitational coupling, suppressed by  $1/M_P$ , the almost continuous spectrum of KK gravitons are summed over and result in a coupling to SM particles suppressed only by powers of  $M_D$ .

The LHC is a useful tool for exploring extra-dimensional scenarios in which the reduced Planck scale is of order several TeV. Note that for such low values of  $M_D$  the ADD scenario with 1 extra dimension is clearly ruled out since it would involve extremely large extra dimensions. For larger values of  $\delta$  however, ADD scenarios are possible.

In this case, the graviton  $G$  is long-lived and invisible to the detector, such that the processes  $Z \rightarrow GZ$  and  $W \rightarrow GW$  give  $Z + \cancel{E}_T$  and  $W + \cancel{E}_T$  final states.

The  $W'$  is a theoretical charged heavy vector boson which can decay to  $WZ$ . If the  $Z$  decays to neutrinos,

it gives the final state of  $W + \cancel{E}_T$ . The production cross section depends on a coupling of the form  $\frac{m_W^2}{m_{W'}^2} \times g_{W'WZ'}$ , meaning the coupling will be inversely proportional to the mass of the  $W'$  boson squared. The  $W'$  may also decay leptonically, although it is not discussed here.

### Experimental Search

The ATLAS experiment at the LHC has placed limits on dark matter production in the  $W + \cancel{E}_T$  channel [19], where the dark matter fields couple to quark initial states and the  $W$  boson has been emitted as initial state radiation. These limits were derived from  $20.3 \text{ fb}^{-1}$  of data produced in  $pp$  collisions at  $\sqrt{s} = 8 \text{ TeV}$ . The full selection is as follows:

- 1 Cambridge-Aachen jet with  $R = 1.2$ ,  $p_T > 250 \text{ GeV}$ ,  $|\eta| < 1.2$ ,  $\sqrt{y} > 0.4$
- $\cancel{E}_T > 350 \text{ GeV}$
- $\leq 1$  narrow jet with  $p_T > 40 \text{ GeV}$ ,  $|\eta| < 4.5$ ,  $\Delta R(\text{narrow jet, fat jet}) > 0.9$
- No electrons, muons, or photons with  $p_T > 10 \text{ GeV}$  and  $|\eta| < 2.47$ ,  $|\eta| < 2.5$ , and  $|\eta| < 2.37$  respectively

The results are consistent with the Standard Model expectation, as shown in Table I.

TABLE I: Data and estimated background yields in the two signal regions, from Ref. [19]. Uncertainties include statistical and systematic contributions.

Process	$\cancel{E}_T > 350 \text{ GeV}$	$\cancel{E}_T > 500 \text{ GeV}$
$Z \rightarrow \nu\bar{\nu}$	$402^{+39}_{-34}$	$54^{+8}_{-10}$
$W \rightarrow \ell^\pm \nu, Z \rightarrow \ell^\pm \ell^\mp$	$210^{+20}_{-18}$	$22^{+4}_{-5}$
$WW, WZ, ZZ$	$57^{+11}_{-8}$	$9.1^{+1.3}_{-1.1}$
$t\bar{t}$ , single $t$	$39^{+10}_{-4}$	$3.7^{+1.7}_{-1.3}$
Total	$707^{+48}_{-38}$	$89^{+9}_{-12}$
Data	705	89

Using the CLs method [23, 24], the ATLAS measurement places an upper limit at 95% confidence level on the cross section within this fiducial region to be  $4.4 \text{ fb}$ , with a typical reconstruction efficiency of 63%.

In order to reinterpret these results in terms of interactions with electroweak bosons, we need only calculate the efficiency of the fiducial region selection for the theory of interest.

### Dark Matter Fiducial Efficiency and Limits

We generate simulated samples of events for each hypothetical signal using MADGRAPH5 [25], with showering

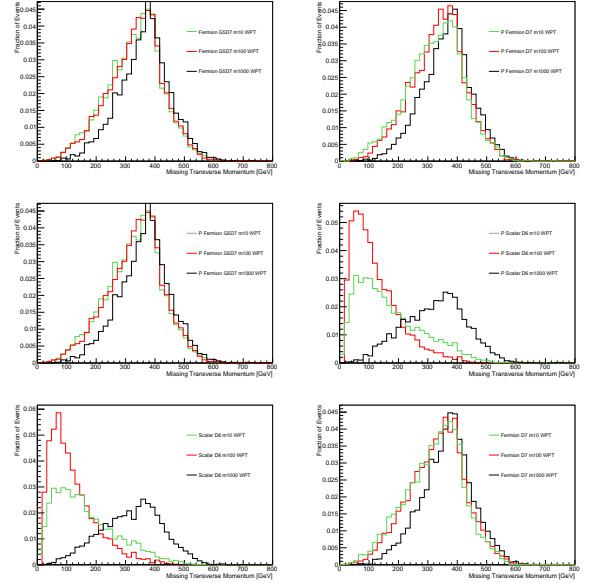


FIG. 2: Distributions of  $\cancel{E}_T$  in simulated  $W\chi\bar{\chi}$  events in  $pp$  collisions at the LHC for several choices of  $m_\chi$ .

and hadronization by PYTHIA [26]. With the exception of the jet-veto requirement, the fiducial efficiency can be reliably estimated using parton-level information.

In each case, the critical kinematic quantity which determines the efficiency is the missing transverse momentum. Figure 2 shows distributions of  $\cancel{E}_T$  in simulated  $W\chi\bar{\chi}$  events for our six effective field theories.

The fiducial efficiencies measured in these simulated samples allow us to calculate limits on the cross section, as shown in Fig. 3 as a function of  $m_\chi$ . As the theoretical cross section depends on the suppression scale  $\Lambda$ , limits on the cross section can be translated into limits on  $\Lambda$ , see Fig. 4.

We observe (Fig. 3) that the limits on light fermionic  $\chi$  are much tighter than those on light scalar  $\phi$  DM, a feature that is obviously due to the differences in  $\cancel{E}_T$  spectra (Fig. 2). It is not hard to understand these differences as, in the limit of massless  $\chi$ , the fact that the fermionic operators are dimension-7 and the scalar operators are dimension-6 means that the cross-sections in the fermionic case must scale with a higher power of the momenta involved<sup>1</sup>, and hence the  $W$ -boson  $p_T$ . The resulting cross-section is relatively suppressed as  $p_T \rightarrow 0$  and is enhanced compared to the scalar case in the large  $p_T$  tail.

<sup>1</sup> Terms that don't scale with momenta are much smaller,  $\mathcal{O}(m_\chi^2)/s$ , i.e., they are “helicity suppressed.”

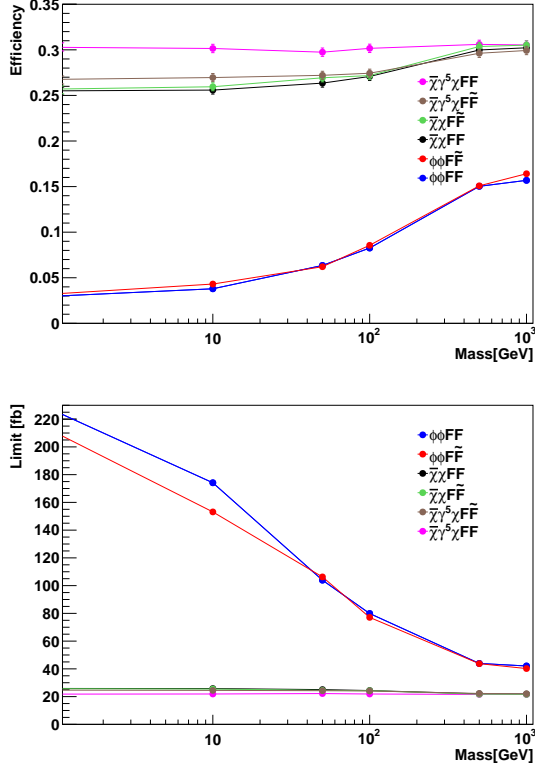


FIG. 3: Fiducial efficiency and limits on  $\sigma(pp \rightarrow W\chi\bar{\chi})$  for several values of  $m_\chi$  for each of the EFTs describing interactions between DM and  $W$  bosons.

### Indirect Signatures from our DM Operators

In addition to collider production of  $W + \cancel{E}_T$ , our operators also mediate DM annihilation into the  $WW$ ,  $ZZ$ ,  $\gamma Z$  and  $\gamma\gamma$  final states. In this section, we convert results from indirect searches into limits on parameters of our EFTs.

The decay products, radiation and hadronization that follows production of the final state bosons generically yields spectral continua of  $\gamma$ -rays, antiprotons, positrons and neutrinos, all of which are long known discovery channels in indirect searches for DM. The latter two processes mediate direct annihilation to  $\gamma$ -rays, giving a highly distinctive monochromatic signal.

In our operator framework, bounds on the scale  $\Lambda$  coming from indirect detection experiments can be directly compared to the collider bounds derived above, provided some important cosmological assumptions. The main assumption here is that our DM makes up *all* of the observed DM density in the universe. This is implicitly assumed in all of the bounds derived below. A useful comparison for this assumption is to keep track of where the DM relic density that *would be* obtained from a thermal freezeout history, (*assuming* that our operator is the dominant annihilation process) matches, exceeds or un-

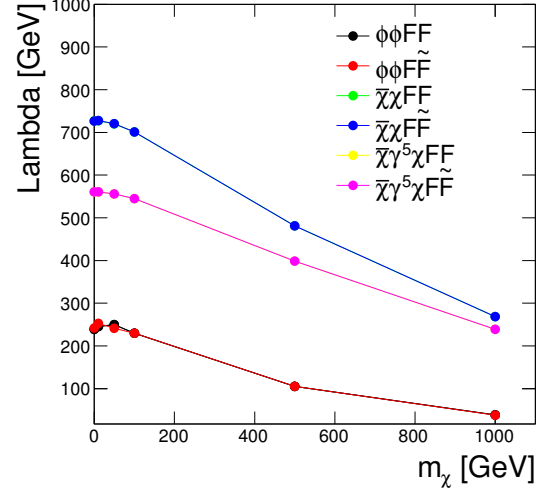


FIG. 4: Limits on  $\Lambda$  as a function of  $m_\chi$ .

dershoots the total relic density of the universe. We provide contours of this thermal relic density calculation below so that we have an idea of where we would need additional structure beyond our model in order to increase or decrease the relic density to match our assumption that our DM makes up all of DM.

We combine the results of several experiments to derive our combined indirect bounds. The analysis closely follows that of [17]. The most robust bounds on continuum  $\gamma$ -rays come from observations of dwarf galaxies. These are extremely low background searches with high-quality estimates for the DM abundance and distributions<sup>2</sup>. We also show bounds coming from the PAMELA antiproton data [27] (using the GALPROP[28][29][30] propagation model galdef\_50p\_599278), although these bounds are relatively weak in comparison to the continuum  $\gamma$ -ray bounds. We use the bounds on the  $WW/ZZ$  annihilation channels derived from the *Fermi*-LAT [31] and VERITAS [32] data, as the two complement each other in  $m_{DM}$ . Bounds on the monochromatic channels are those from the *Fermi*-LAT work [33] and assume an NFW profile for the galactic DM distribution (this is not as robust an assumption as in the dwarf limits). The resulting bounds from indirect detection are shown for the  $B_{1,2}$  operators in Fig. 5.

We do not consider continuum  $\gamma$ -ray bounds from the galactic center (as they are exquisitely sensitive to the DM distribution) or bounds from neutrino telescopes

<sup>2</sup> we use limits that assume an NFW profile for the dwarf DM distribution, but these kinds of searches (being sensitive to the integral of DM density squared over the entire distribution) are relatively insensitive to this assumption.

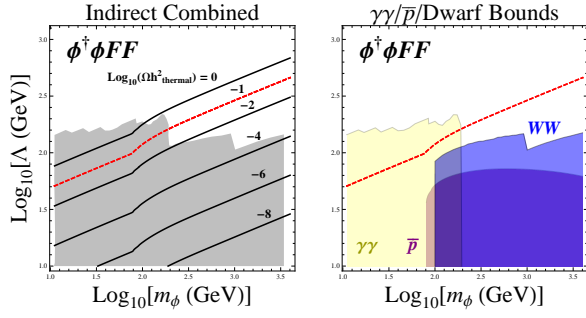


FIG. 5: Bounds on the the  $B_{1,2}$  operators from indirect detection searches for annihilation. Here  $k_1 = k_2$  so there is no bound from the monochromatic  $\gamma Z$  channel. Shown are the constraints on the  $\gamma\gamma$  channel from the LAT line search, on the  $WW$  channel from dwarf bounds on continuum  $\gamma$ 's and from the PAMELA  $\bar{p}$  data. The black and red-dashed curves indicate the relic density that would be obtained from a thermal calculation assuming this operator is the dominant process in freezeout. The picture is qualitatively similar for the other operators so similar figures are omitted.

(bounds from the galactic center are not competitive, while bounds from the solar DM search must rely on additional assumptions about how our DM scatters on SM particles). There are no bounds from the  $\gamma Z$  channel in our plots as this channel is turned off for the custodially-symmetric combination  $k_1 = k_2$ . Away from this special case the *Fermi*-LAT  $\gamma Z$  bound would be a non-trivial constraint, however, we simply note here that the reach would be much the same (and overlapping in  $m_{DM}$ ) as the  $\gamma\gamma$  bound.

Figures 6-8 compare the limits that can be derived for our effective operators from the collider and indirect searches employed in this work. The most obvious feature of these plots is the disparity in collider and indirect reaches for operators  $C_{1-4}$ , a result of the velocity suppression of the bilinear  $\bar{\chi}\chi$ . Aside from this the collider and indirect reaches are seen to be comparable, and highly complementary over the range of  $m_\chi$  considered here.

### Heavy Boson Fiducial Efficiency and Limits

The fiducial efficiency for  $W \rightarrow GW$  and  $Z \rightarrow GZ$  as a function of number of extra dimensions  $\delta$  for the ADD model can be found in Fig. 9(a). We find no significant difference for various  $M_D$  values, so quote a single number for each  $\delta$ .

As above, the efficiencies allow the derivation of limits on the cross section, see Fig. 9(b). These limits can be converted into limits on  $M_D$  according to this relationship  $\sigma \sim 1/M_D^{\delta+2}$ , see Table II. The current limits are also listed [34].

The most stringent current limits on  $M_D$  in the ADD

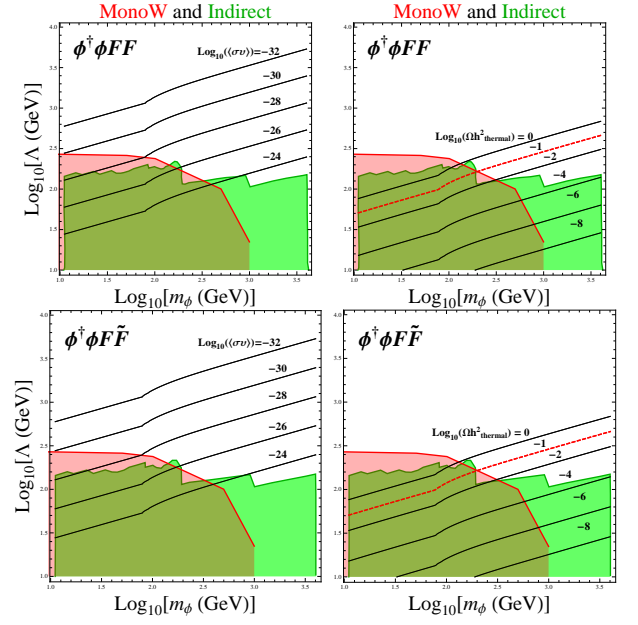


FIG. 6: Comparison of constraints on the  $B_{1,2}$  and  $B_{3,4}$  operators coming from the collider  $W + \cancel{E}_T$  search (red) and indirect searches (green). Curves describing current annihilation cross-sections and thermal relic density are shown in the left and right panels, respectively.

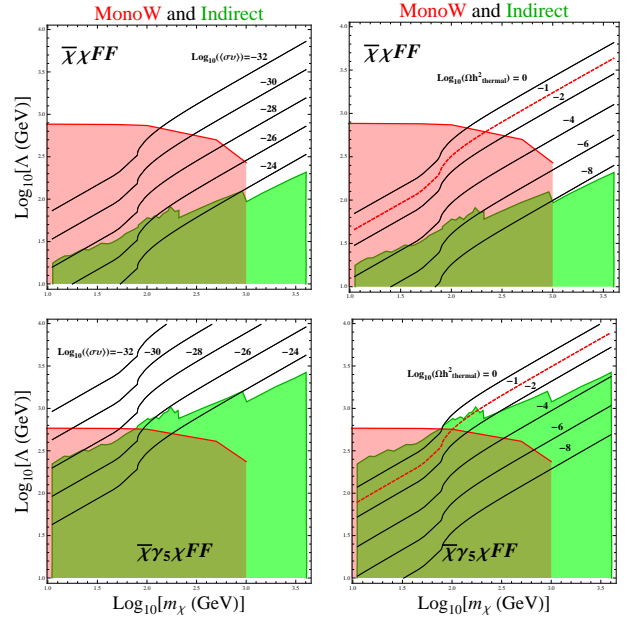


FIG. 7: As in Fig. 6 for the  $C_{1,2}$  and  $C_{5,6}$  operators.

scenario come from CMS mono-jet searches [7]. Our result is the first constraint on ADD derived in the mono- $W$  channel and it is competitive with other hadron collider limits on  $M_D$  in electroweak channels. For example, CDF's mono-photon search for  $\delta = 2$  places a limit on  $M_D$  of 1.39 TeV [35].

In the case of the  $W'$  boson, the selection efficiency is

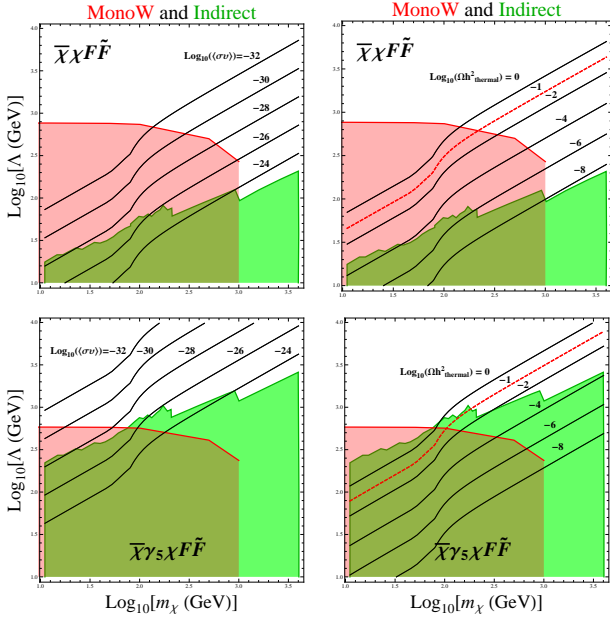


FIG. 8: As in Fig. 6 for the  $C_{3,4}$  and  $C_{7,8}$  operators.

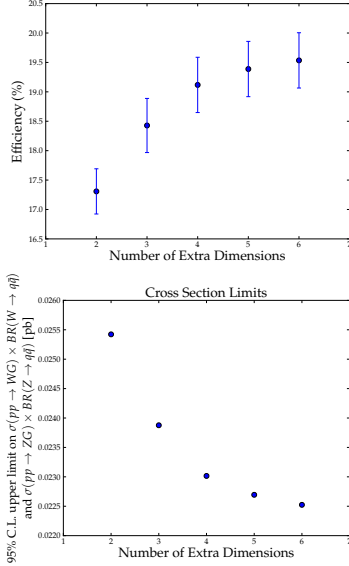


FIG. 9: For ADD [21] models predicting  $WG$  or  $ZG$  production, fiducial selection efficiency (top) and cross-section limits (bottom).

a strong function of the  $W'$  boson mass, as the missing transverse energy is due to the  $p_T$  of the  $Z$  boson, which is approximately half of the  $W'$  boson mass. The efficiency and cross section limits derived from it can be found in Fig. 10.

This excludes  $W'$  masses between 823 and 1055 GeV. This exclusion is the first for this scenario in the  $W + \cancel{E}_T$  channel, and are a good complement to other search channels for fermiophobic scenarios. Current limits on

TABLE II: Limits on  $M_D$  at 95% CL calculated from limits on cross section in Fig. 9(b) for each number of extra dimensions, along with the current limits on  $M_D$  [34].

Number of Extra Dimensions	Our Limits $M_D$ (TeV/ $c^2$ )	Current Limits (TeV/ $c^2$ )
2	1.84	5.67
3	1.85	4.29
4	1.89	3.71
5	1.92	3.31
6	1.96	3.12

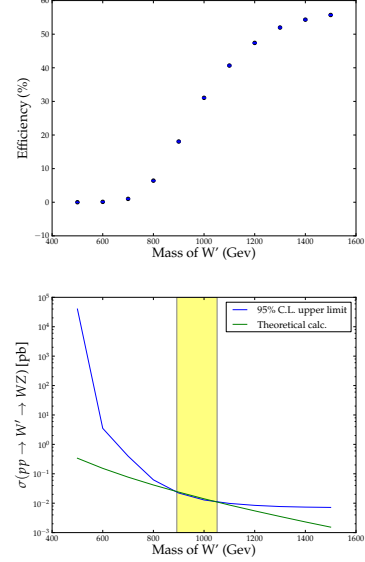


FIG. 10: For models predicting  $pp \rightarrow W' \rightarrow WZ$ , fiducial selection efficiency (top) and cross-section limits for several values of  $m_{W'}$  (bottom).

$W'$  scenarios with large direct coupling to fermion are quite restrictive: 2.6 TeV for the  $\ell\nu$  channel and 1.9 TeV for the  $q\bar{q}$  [35]. However, limits in fermi-phobic scenarios are substantially more relaxed. The most stringent limit is from CMS who searched in the multi-lepton channel  $pp \rightarrow W' \rightarrow WZ$  where  $W \rightarrow \ell\nu$  and  $Z \rightarrow \ell\ell$ ; in the sequential SM scenario the mass exclusion is 1.143 TeV [36] assuming  $g_{W'WZ}/g_{WWZ} = (m_W/m_{W'})^2$ . The ATLAS collaboration search in the same channel yielded a limit of 760 GeV[37].

## Conclusions

In this work we have derived constraints on dark matter interactions with  $W$  bosons in the context of a simply parameterized effective theory framework.  $W + \cancel{E}_T$  bounds derived by the ATLAS collaboration for dark matter interactions with quarks were recast to find bounds on our model for both scalar and fermionic dark



matter scenarios, and compared to limits derived from indirect experiments. We note that due to gauge invariance effective operators considered in this analysis which couples dark matter to pairs of  $W$  bosons must also predict non-zero coupling to of dark matter to other pairs of gauge bosons. Thus we expect mono- $W$  search constraints may be combined with other searches, for example mono-photons, to increase the power of the effective operator analysis.

We have additionally pointed out that the  $W + \cancel{E}_T$  have sensitivity in to heavy boson theories. We give results in terms of an ADD model of extra dimensions to produce limits on cross section and graviton coupling to  $W$ , placing lower limits on  $M_D$  between 1.84 and 1.96 TeV. We analyze  $W'$  production to give the first limits on this model in this final state, excluding  $W'$  masses between 823 and 1055 GeV.

### Acknowledgements

We acknowledge useful conversations with Tim Tait. DW and NZ are supported by grants from the Department of Energy Office of Science. RC was supported in part by the National Science Foundation under PHY-0970173 and PHY11-25915.

- 
- [1] G. Bertone, D. Hooper, J. Silk, Phys. Rept. **405**, 279 (2005) [arXiv:0404175 [hep-ph]].
  - [2] P. A. R. Ade *et al.* [Planck Collaboration], arXiv:1303.5076 [astro-ph.CO].
  - [3] D. S. Akerib *et al.* [LUX Collaboration], arXiv:1310.8214 [astro-ph.CO].
  - [4] E. Aprile *et al.* [XENON100 Collaboration], Phys. Rev. Lett. **109**, 181301 (2012) [arXiv:1207.5988 [astro-ph.CO]].
  - [5] [Fermi-LAT Collaboration], Physical Review D **88**, **082002** (2013) [arXiv:1305.5597 [astro-ph.HE]].
  - [6] G. Aad *et al.* [ATLAS Collaboration], JHEP **1304**, 075 (2013) [arXiv:1210.4491 [hep-ex]].
  - [7] S. Chatrchyan *et al.* [CMS Collaboration], JHEP **1209**, 094 (2012) [arXiv:1206.5663 [hep-ex]].
  - [8] G. Aad *et al.* [ATLAS Collaboration], arXiv:1209.4625 [hep-ex].
  - [9] S. Chatrchyan *et al.* [CMS Collaboration], Phys. Rev. Lett. **108**, 261803 (2012) [arXiv:1204.0821 [hep-ex]].
  - [10] J. Goodman, M. Ibe, A. Rajaraman, W. Shepherd, T. M. P. Tait and H. -B. Yu, Phys. Rev. D **82**, 116010 (2010) [arXiv:1008.1783 [hep-ph]].
  - [11] M. Beltran, D. Hooper, E. W. Kolb, Z. A. C. Krusberg and T. M. P. Tait, JHEP **1009**, 037 (2010) [arXiv:1002.4137 [hep-ph]].
  - [12] P. J. Fox, R. Harnik, J. Kopp and Y. Tsai, Phys. Rev. D **85**, 056011 (2012) [arXiv:1109.4398 [hep-ph]].
  - [13] N. Zhou, D. Berge and D. Whiteson, arXiv:1302.3619 [hep-ex].
  - [14] L. M. Carpenter, A. Nelson, C. Shimmin, T. M. P. Tait and D. Whiteson, arXiv:1212.3352 [hep-ex].
  - [15] N. F. Bell, J. B. Dent, A. J. Galea, T. D. Jacques, L. M. Krauss and T. J. Weiler, Phys. Rev. D **86**, 096011 (2012) [arXiv:1209.0231 [hep-ph]].
  - [16] A. Nelson, L. M. Carpenter, R. Cotta, A. Johnstone and D. Whiteson, arXiv:1307.5064 [hep-ph].
  - [17] R. C. Cotta, J. L. Hewett, M. P. Le and T. G. Rizzo, arXiv:1210.0525 [hep-ph].
  - [18] A. Rajaraman, T. M. P. Tait and A. M. Wijangco, arXiv:1211.7061 [hep-ph].
  - [19] G. Aad *et al.* [ATLAS Collaboration], arXiv:1309.4017 [hep-ex].
  - [20] L. Randall and R. Sundrum, Phys. Rev. Lett. **83**, 3370 (1999) [hep-ph/9905221].
  - [21] N. Arkani-Hamed, S. Dimopoulos and G. R. Dvali, Phys. Lett. B **429**, 263 (1998) [hep-ph/9803315].
  - [22] G. Altarelli, B. Mele and M. Ruiz-Altaba, Z. Phys. C **45**, 109 (1989) [Erratum-ibid. C **47**, 676 (1990)].
  - [23] A. Read, J. Phys. G: Nucl. Part. Phys. **28**, 2693 (2002);
  - [24] T. Junk, Nucl. Instrum. Methods A **434**, 425 (1999).
  - [25] J. Alwall, M. Herquet, F. Maltoni, O. Mattelaer and T. Stelzer, JHEP **1106**, 128 (2011) [arXiv:1106.0522 [hep-ph]].
  - [26] T. Sjostrand, S. Mrenna and P. Z. Skands, JHEP **0605**, 026 (2006) [hep-ph/0603175].
  - [27] O. Adriani *et al.* [PAMELA Collaboration], Phys. Rev. Lett. **105**, 121101 (2010) [arXiv:1007.0821 [astro-ph.HE]].
  - [28] A. W. Strong and I. V. Moskalenko, Astrophys. J. **509**, 212 (1998) [astro-ph/9807150].
  - [29] I. V. Moskalenko, A. W. Strong, J. F. Ormes and M. S. Potgieter, Astrophys. J. **565**, 280 (2002) [astro-ph/0106567].
  - [30] <http://galprop.stanford.edu>
  - [31] M. Ackermann *et al.* [Fermi-LAT Collaboration], Phys. Rev. Lett. **107**, 241302 (2011) [arXiv:1108.3546 [astro-ph.HE]].
  - [32] E. Aliu *et al.* [VERITAS Collaboration], Phys. Rev. D **85**, 062001 (2012) [arXiv:1202.2144 [astro-ph.HE]].
  - [33] M. Ackermann *et al.* [LAT Collaboration], arXiv:1205.2739 [astro-ph.HE].
  - [34] CMS Note PAS-EXO-12-048 [CMS Collaboration].
  - [35] J. Beringer *et al.* [Particle Data Group], Phys. Rev. D **86**, 010001 (2012).
  - [36] S. Chatrchyan *et al.* [CMS Collaboration], Phys. Rev. Lett. **109**, 141801 (2012) [arXiv:1206.0433 [hep-ex]].
  - [37] G. Aad *et al.* [ATLAS Collaboration], Phys. Rev. D **85**, 112012 (2012) [arXiv:1204.1648 [hep-ex]].